

From Liquid Crystals Localized Modes to Localized Modes in Photonic Crystals

Belyakov VA*

Landau Institute for Theoretical Physics, Moscow, Russia

Recently a great attention was paid to the localized optical modes in photonic liquid crystals (PLC) due to the perspectives of their efficient application in the linear and nonlinear optics [1,2]. Luckily, an analytic description of the localized modes is available for PLC due to their spiral structure [3,4]. The purpose of this paper is to attract attention to the fact that many results obtained analytically for PLC are also applicable to the conventional photonic crystals and the corresponding simple formulas may be useful in the description of the localized modes in conventional photonic crystals. So, below are given main relationships for the edge localized modes (EM) in PLC and discussed the options of their application for describing EM in conventional photonic crystals (Figure 1).

For describing EM in chiral liquid crystals (CLC), for the certainty it will be assumed that CLC is used for cholesteric liquid crystals, one has to solve an optical boundary problem for a perfect CLC layer (Figure 1). The solution of the boundary problem [3] results in the following expressions for the amplitude reflection and transmission coefficients for a layer of thickness L (it is assumed that the spiral axis of CLC is normal to the layer surfaces and light of the circular polarization of the same sense of chirality as the one of CLC spiral propagates along this axis):

$$R(L) = \delta \sin qL / \{ (q\tau/\kappa^2) \cos qL + i [(\tau/2\kappa)^2 + (q/\kappa)^2 - 1] \sin qL \} \quad (1a)$$

$$T(L) = \exp[i\kappa L] (q\tau/\kappa^2) / \{ (q\tau/\kappa^2) \cos qL + i [(\tau/2\kappa)^2 + (q/\kappa)^2 - 1] \sin qL \} \quad (1b)$$

where

$$q = k \{ 1 + (\tau/2k)^2 - [(\tau/k)^2 + \delta^2]^{1/2} \}^{1/2} \text{ and } \epsilon = (\epsilon_{\parallel} + \epsilon_{\perp}) / 2, \delta = (\epsilon_{\parallel} - \epsilon_{\perp}) / (\epsilon_{\parallel} + \epsilon_{\perp})$$

Here δ is the dielectric anisotropy of CLC with ϵ_{\parallel} and ϵ_{\perp} as the local principal values of the CLC dielectric tensor [3], $k = \omega \epsilon_0^{1/2} / c$ with c as the speed of light, and $\tau = 4\pi/p$ with p as the cholesteric pitch.

The frequencies of reflection coefficient minima (Figure 2) which may be numerated by integer numbers n [4] determine the real part of the EM frequency ω_{EM} .

The imaginary part of EM frequency $\omega_{EM} = \omega(1+i\Delta)$ where Δ is a small parameter can be found from the dispersion equation [4] which in a general case demands a numerical approach for its solution. The EM energy is localized inside the layer (with the number of energy density maxima inside the layer coinciding with the EM number n). For thick layers the dispersion equation determining via the imaginary part of EM frequency the EM life-time may be solved analytically:

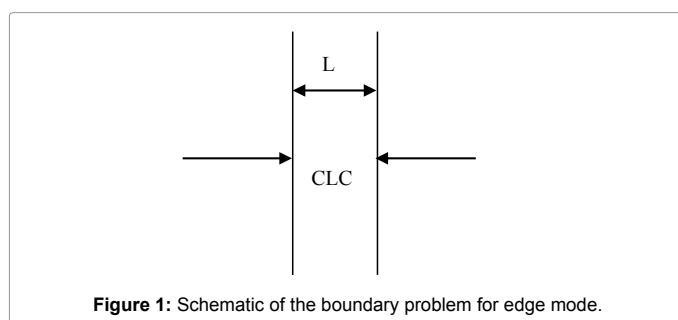


Figure 1: Schematic of the boundary problem for edge mode.

$$\Delta = - \frac{1}{2} \delta (n\pi)^2 / (\delta L \tau / 4)^3 \quad (2)$$

I.e., the EM life-time for non-absorbing CLC is proportional to the third power of the layer thicknesses.

At the EM frequency effects of anomalously strong absorption or amplification exist for absorbing or amplifying CLC [5]. It is why, in particular, the observed lasing threshold at the EM frequency occurs to be lower than (Figure 2) for lasing in the corresponding homogeneous layer [1,2,5]. The lasing threshold value is determined by a minimal value of the negative imaginary addition to the dielectric constant $\epsilon_0(1-i)$, (with γ being determined by the population inversion in the lasing transition) ensuring the lasing. In a general case γ can be found from the dispersion equation. However, for a thick layer the threshold values of the gain (γ) for the EM can be presented by the analytic expression [4]:

$$\gamma = - \delta (n\pi)^2 / (\delta L \tau / 4)^3 \quad (3)$$

The equation (3) shows that the lasing threshold at the EM frequency is inversely proportional to the third power of the layer thickness L and formally approaches to zero with a growing L (naturally, the decreasing of γ according (3) is limited by the CLC absorption [6]).

The experimentally observed enhancement of some optical effects in CLC at the EM frequency (lowering of the lasing threshold, abnormally strong absorption etc.) described by the presented above

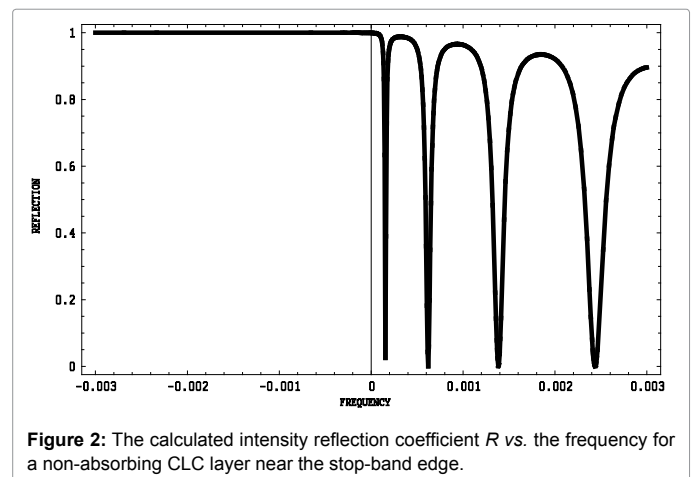


Figure 2: The calculated intensity reflection coefficient R vs. the frequency for a non-absorbing CLC layer near the stop-band edge.

*Corresponding author: Belyakov VA, Landau Institute for Theoretical Physics, Moscow, Russia, Tel: +7 499 137-32-44; E-mail: bel@landau.ac.ru

Received April 25, 2017; Accepted April 29, 2017; Published May 10, 2017

Citation: Belyakov VA (2017) From Liquid Crystals Localized Modes to Localized Modes in Photonic Crystals. J Laser Opt Photonics 4: 153. doi: [10.4172/2469-410X.1000153](https://doi.org/10.4172/2469-410X.1000153)

Copyright: © 2017 Belyakov VA. This is an open-access article distributed under the terms of the Creative Commons Attribution License, which permits unrestricted use, distribution, and reproduction in any medium, provided the original author and source are credited.

analytic theory [4,6] is also observed for conventional photonic crystals [7-11]. However, a theoretical numerical approach is usually applied for interpreting the experiment and as a result rather frequently the physics of studied phenomenon remains not completely clear. To the mentioned above phenomena enhanced at the EM frequency one can add a nonlinear frequency conversion, sum frequency generation, Cherenkov radiations etc. In general, the situation with the theoretical description of localized mode effects in conventional photonic crystals appears as follows. Almost all publications reporting experimental results on the localized modes are accompanied by numerical calculations of the measured quantities showing a good agreement with the measured results. However, a clear physical image of the observed phenomenon is often escaping the theoretical interpretation of the observed results and the most often the explanation is of the type “the effect is enhanced near to the stop-band edge”. It is why due to the common physics of the localized mode effects in CLC and conventional photonic crystals the analytic theory developed for CLC can be applied for conventional photonic crystals as a qualitative guide for a qualitative description of the experiment and clearing the physics of phenomenon.

As examples, below some enhanced, due to the EM, phenomena experimentally observed in conventional photonic crystals [9-11] are mentioned and the interpretation related to the localized modes for one example is proposed. We mention enhancement phenomena in conventional photonic crystals for the second nonlinear harmonic generation (SHG) [10], third nonlinear harmonic generation (THG) [12] and sum frequency generation [11] where the enhancement effects at the stop-band edge frequency are attributed to the decrease of the

light group velocity, increase of the density of states and to the growth of wave field at this frequency [7-9] (Figure 3).

The enhancement of SHG generation in a ZnS-SrF₂ periodic structure near the photonic band edge [10] was observed at applying to the sample of femtosecond laser pumping pulses. The SHG was measured as a function of the pumping wave incidence angle. The SHG intensity enhancement observation (Figure 3) just corresponded to the pumping wave incidence angle coinciding with the first minimum in the linear reflection curve for the pumping frequency. As the estimate shows this angle just corresponds to the first EM frequency coinciding with the pumping frequency so the enhancement can be interpreted in the terms of EM as a result of anomalously strong absorption of the pumping wave.

We considered here the enhancement phenomena related to the localized edge modes. Similar effects are also happening for other types of localized modes, for example, localized defect modes [12]. So, in conclusion should be emphasized that the presented for localized modes in CLC results are of a general nature and are qualitatively applicable for different localized modes in various structures.

Funding

The work is supported by the RFBR grants № 16-02-00679_a and № 16-02-00295_a.

References

1. Blinov LM, Bartolino R (2010) *Liquid Crystals Microlasers*. Physical Sciences.
2. Kopp VI, Zhang ZQ, Genack AZ (2003) *Prog Quantum Electron*. **27**: 369
3. Belyakov VA, (1992) *Diffraction Optics of Complex Structured Periodic Media*, Springer Verlag, New York.
4. Belyakov VA, Semenov SV (2009) Localized modes in optics of photonic liquid crystals with local anisotropy of absorption. *JETP* 149: 1076.
5. Chigrinov VG (2013) *New Developments in Liquid Crystals and Applications*. Choudhury PK editor. Nova Publishers, New York, pp: 199-227.
6. Belyakov VA, Semenov SV (2016) Localized modes in optics of photonic liquid crystals with local anisotropy of absorption. *JETP* 122: 932-941.
7. Dowling JP, Scalora M, Bloemer MJ, Bowden CM. (1994) The photonic band edge optical diode. *J Appl Phys* 75: 1896.
8. Scalora M, Bloemer MJ, Manka AS, Dowling JP, Bowden CM et al. (1997) Pulsed second-harmonic generation in nonlinear, one-dimensional, periodic structures. *Phys Rev A* 56: 3166.
9. Balakin AV, Bushuev VA, Koroteev NI, Mantsyzov IA, Ozheredov AP et al. (1999) Enhancement of second-harmonic generation with femtosecond laser pulses near the photonic band edge for different polarizations of incident light. *Opt Lett* 24: 793-795.
10. Balakin AV, Bushuev VA, Mantsyzov BI, Ozheredov EV, Petrov AP et al. (2001) Enhancement of sum frequency generation near the photonic band gap edge under the quasiphase matching conditions. *Phys Rev E* 63: 046609.
11. Dolgov T, Didenko NV, Martem'yanov MG, Aktsipertov OA, Marowsky G, et al. (2002) Third-harmonic generation in silicon photonic crystals and microcavities. *IEEE Xplore* 75:17.
12. Belyakov VA, Semenov SV (2011) Optical defect modes in chiral liquid crystals. *JETP* 112: 694.

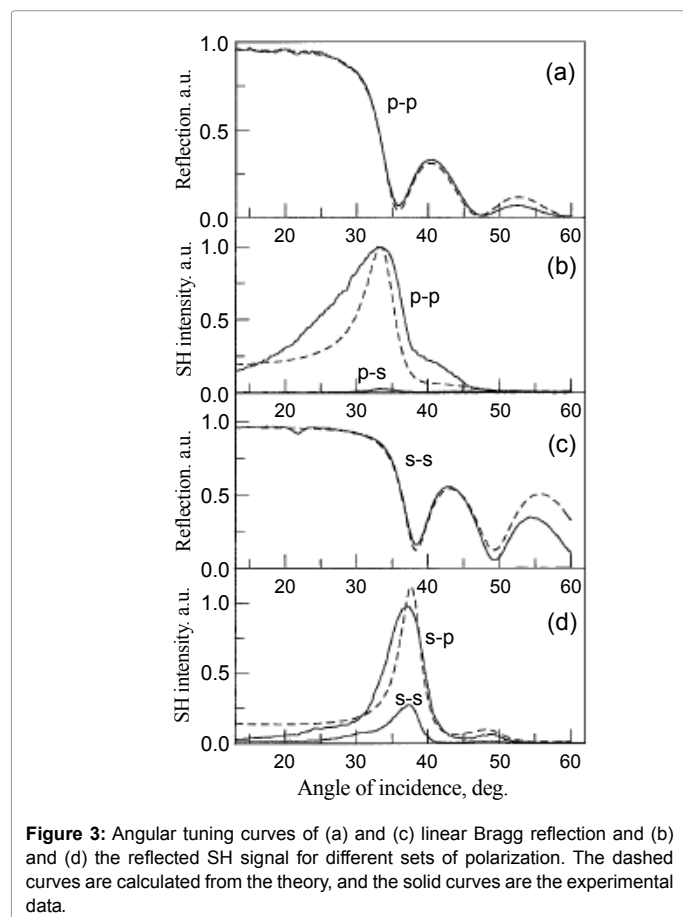


Figure 3: Angular tuning curves of (a) and (c) linear Bragg reflection and (b) and (d) the reflected SH signal for different sets of polarization. The dashed curves are calculated from the theory, and the solid curves are the experimental data.